Determination of p-y Curves for Bucket Foundations in Silt and Sand Using Finite Element Modelling

Vethanayagam, Vinojan; Ibsen, Lars Bo

Publication date:
2017

Document Version
Publisher's PDF, also known as Version of record

Determination of p-y Curves for Bucket Foundations in Silt and Sand Using Finite Element Modelling

Vinojan Vethanayagam
Lars Bo Ibsen

ISSN 1901-7278
DCE Technical Memorandum No. 64

Aalborg University
Department of Civil Engineering

DCE Technical Memorandum No. 64

Determination of p-y Curves for Bucket Foundations in Silt and Sand Using Finite Element Modelling

by

Vinojan Vethanayagam
Lars Bo Ibsen

June 2017

Scientific Publications at the Department of Civil Engineering

Technical Reports are published for timely dissemination of research results and scientific work carried out at the Department of Civil Engineering (DCE) at Aalborg University. This medium allows publication of more detailed explanations and results than typically allowed in scientific journals.

Technical Memoranda are produced to enable the preliminary dissemination of scientific work by the personnel of the DCE where such release is deemed to be appropriate. Documents of this kind may be incomplete or temporary versions of papers—or part of continuing work. This should be kept in mind when references are given to publications of this kind.

Contract Reports are produced to report scientific work carried out under contract. Publications of this kind contain confidential matter and are reserved for the sponsors and the DCE. Therefore, Contract Reports are generally not available for public circulation.

Lecture Notes contain material produced by the lecturers at the DCE for educational purposes. This may be scientific notes, lecture books, example problems or manuals for laboratory work, or computer programs developed at the DCE.

Theses are monograms or collections of papers published to report the scientific work carried out at the DCE to obtain a degree as either PhD or Doctor of Technology. The thesis is publicly available after the defence of the degree.

Latest News is published to enable rapid communication of information about scientific work carried out at the DCE. This includes the status of research projects, developments in the laboratories, information about collaborative work and recent research results.

Published 2017 by
Aalborg University
Department of Civil Engineering
Thomas Manns Vej 23,
DK-9220 Aalborg SV, Denmark

Printed in Aalborg at Aalborg University

ISSN 1901-7278
DCE Technical Memorandum No. 64

Determination of p-y Curves for Bucket Foundations in Silt and Sand Using Finite Element Modelling

Vinojan Vethanayagam[1] Lars Bo Ibsen[2]

Department of Civil Engineering, Aalborg University

Abstract

Design of offshore wind turbine foundations are today based on analytical formulas, which describes the link between a displacement, y, and the associated soil pressure, p. The formulas are empirically developed on slender piles with a slenderness ratio $L/D > 30$, but foundations of today are less slender than the tested piles. The suction bucket has a slenderness ratio of 0.5-1, thus its response is a rigid movement, where slender piles undergoes a flexible movement. Due to the importance of precise estimations, p-y formulations for suction buckets in drained and undrained silt are sought developed with use of finite element. In general the developed p-y formulations for the drained and undrained silt are fairly precise. Furthermore, the same method and basic formulation of the drained silt is applied to data of the drained sand from Østergaard et al. [2015]. The developed formulation herefore shows to be more versatile and precise than the formulation suggested by Østergaard et al. [2015]. The developed p-y formulations are functions of the effective vertical in-situ stress, soil stiffness, diameter of the bucket and the internal friction angle/the undrained shear strength.

1 Introduction

The empirically developed p-y curves are the analytical design tool for offshore foundations of today, which are recommended by the offshore design code, Det Norske Veritas [2013]. The piles used in the conducted field tests were small-diameter piles, which had slenderness ratios of $L/D > 30$. Matlock [1970] developed the suggested p-y curves for piles in clay by conducting tests in Lake Austin, USA with use of piles with $L = 12.8$ m and $D = 0.32$ m, while p-y curves for sand were formulated by Cox et al. [1974], where the tests were conducted at Mustang Island, USA with $L = 21$ m and $D = 0.61$ m piles.

Since the p-y curves were developed from small-diameter and slender piles, problems are introduced, when they are used to design foundations for wind turbines of today. Wind turbines gets bigger to cut the costs, thereby the foundations are also becoming bigger, hence the slenderness ratios are far less than piles from Matlock [1970] and Cox et al. [1974]. Monopiles and suction buckets are two foundations type, which are used offshore, and they behave significantly different from slender piles, as $L/D \approx 5$ and 0.5-1 respectively. As seen in Figure 1, slender piles, such as the piles from Matlock [1970] and Cox et al. [1974], have a flexible response, while less slender piles, such as a monopile or suction bucket, have a more rigid response. Therefore, the p-y curves suggested in Det Norske Veritas [2013] are not precise, and it is possible to cut costs by introducing p-y curves valid for non-slender piles such as monopiles and suction buckets.

Thieken et al. [2015] modelled monopiles in sand using finite element, from which the soil-structure interaction were simulated. Hence it was possible to develop p-y curves valid for monopiles in sand. Achmus et al. [2016] made a similar study for clay, where the p-y curves have not yet been developed, but are sought in a similar manner as in Thieken et al. [2015].

Even though monopiles and suction buckets both are considered non-slender piles, the slenderness ratio is significantly different. Thus, it would be favourable to develop p-y curves for suction buckets using finite element as well. Østergaard et al. [2015] studied suction buckets in drained sand with use of finite element, and developed a p-y formulation, which estimates the soil pressure fairly well.

In continuation of Østergaard et al. [2015], this article will develop p-y curves for suction buckets in drained and undrained silt using finite element by modelling a number of numerical models to simulate the soil-structure interaction. The formulation has to be simple and practically applicable without comprising on the precision. As it is in continuation of Østergaard et al. [2015], the formulation are sought to be similar in many senses. However, some elements of the formulation will be different, as Vahdatirad et al. [2016] used the formulation by Østergaard et al. [2015] in an analytical calculation, which were compared to data from a field test of a suction bucket. Here it was seen, that the small-strain response of the analytical model was softer than obtained in field test. Vahdatirad et al. [2016] concluded, it might be caused by the model parameters, β_{1-4}, which control the shape of the load-displacement response. Thus, this

[1] *M.Sc. Student, Department of Civil Engineering, Aalborg University, Denmark*

[2] *Professor, Department of Civil Engineering, Aalborg University, Denmark*

article will implement the soil stiffness as a governing parameter for the model parameters instead of the friction angle.

Since the data from Østergaard et al. [2015] is available, and it is assumed, that the model parameters cause imprecise predictions of the soil pressure, the p-y formulation for suction buckets in drained sand will be reconsidered in this article by developing a formulation similar to the silt.

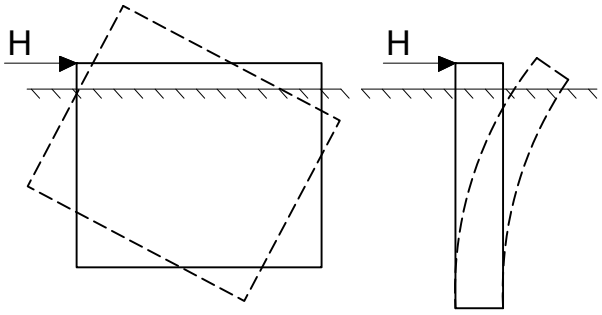

Figure 1: Response of non-slender and slender pile to a horizontal load.

2 Material Model

The numerical models will be defined with the use of the Hardening Soil Small Strain (HSsmall) material model. The HSsmall model is a sophisticated material model due to its interpretation capabilities of advanced soil behaviour. It takes hardening into account as the stiffness moduli are stress-dependent, thus value for each stiffness moduli are given at a reference pressure at p^{ref} = 100 kPa. The stiffness moduli in the HSsmall model changes according to the current stress-state of the soil with use of a power law with the exponent m, and they are given in Eq. (1). Furthermore, the material model also take the additional stiffness at small strains into account, hence the model is capable of simulating real-life behaviour of the soil-structure interaction relatively well.

$$\begin{aligned} E_{oed} &= E_{oed}^{ref} \cdot \left(\frac{c \cdot \cos\phi + \sigma_1' \cdot \sin\phi}{c \cdot \cos\phi + p^{ref} \cdot \sin\phi} \right)^m \\ E_{50} &= E_{50}^{ref} \cdot \left(\frac{c \cdot \cos\phi + \sigma_3' \cdot \sin\phi}{c \cdot \cos\phi + p^{ref} \cdot \sin\phi} \right)^m \\ E_{ur} &= E_{ur}^{ref} \cdot \left(\frac{c \cdot \cos\phi + \sigma_3' \cdot \sin\phi}{c \cdot \cos\phi + p^{ref} \cdot \sin\phi} \right)^m \\ G_0 &= G_0^{ref} \cdot \left(\frac{c \cdot \cos\phi + \sigma_3' \cdot \sin\phi}{c \cdot \cos\phi + p^{ref} \cdot \sin\phi} \right)^m \end{aligned} \quad (1)$$

The calculation time is considered high, when using the HSsmall model, due to its advanced interpretation capabilities. Nevertheless, the material model allows to both take hardening of the soil and the small strain stiffness into account, which are considered utmost important to find the link between displacement, y, and the associated soil pressure, p. Thus the extra calculation time is well spend.

3 Determination of Input Parameters

As both drained and undrained silt are considered in the study, the modelling of the numerical models are different between these two types. The drained models are simply modelled as drained, where both strength and stiffness parameters are defined effective. On the other hand, the stiffness parameters are effective, while strength parameters are total for the undrained models, as they are modelled with use of Undrained (B) as in Achmus et al. [2016], which allows to define the undrained shear strength, c_u, as an input parameter.

The input parameters for the numerical models are given in Table 2, where two types of silts are used and denoted as soft and stiff silt. To model the silt with the HSsmall material model, G_0 and $\gamma_{0.7}$ have to be determined, furthermore the c_u for the soft and stiff silt has to be defined as well.

3.1 Determination of Shear Modulus and Threshold Shear Strain

G_0 and $\gamma_{0.7}$ are found with use of Det Norske Veritas [1992], where a relation between the modulus no., m, and the porosity, n, is given, where m is defined in intervals of:

Loose:	m = 40 - 60
Medium:	m = 60 - 80
Dense:	m > 80

With use of the above-mentioned intervals and the relation given in Figure 2, G_0 and $\gamma_{0.7}$ are obtained by Eq. (2) from Brinkgreve et al. [2015].

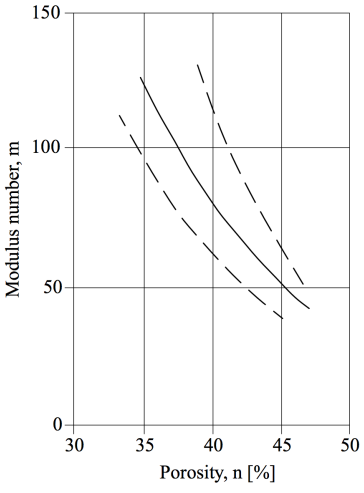

Figure 2: Relation between modulus no., m, and porosity, n, [Det Norske Veritas, 1992, Fig. 5.9, Sec. 5.3.3.8].

$$\begin{aligned} G_0^{ref} &= 33 \cdot \frac{(2.97 - e)^2}{1 + e} \\ \gamma_{0.7} &= \frac{2\text{c'}\,(1 + \cos(2\phi')) - \sigma_1'(1 + K_0)\sin(2\phi)}{9G_0} \end{aligned} \quad (2)$$

3.2 Determination of Undrained Shear Strength

In PLAXIS it is possible to perform undrained triaxial tests with a soil defined with effective strength and stiffness parameters. Thus, the SHANSEP method is used to determine c_u.

The SHANSEP formula is given in Eq. (3), where $(c_u/\sigma'_1)_{nc}$ is the only unknown part of the equation. It is obtained by performing consolidated undrained (CU) triaxial tests at different values of OCR. Since the consolidation phase of the triaxial tests is performed with K_0-consolidation, Λ is set to 0.8, as recommended by Jensen et al. [2015]. Results from all the triaxial tests is shown in Table 1.

$$\left(\frac{c_u}{\sigma'_1}\right)_{oc} = \left(\frac{c_u}{\sigma'_1}\right)_{nc} \cdot OCR^{\Lambda} \tag{3}$$

The necessary input parameters, which are needed to define the soft and stiff silt as drained and undrained HSsmall materials, are given in Table 2.

Table 1: Triaxial test results.

OCR [−]	$\sigma'_{1,nc}$ [kPa]	$\sigma'_{3,nc}$ [kPa]	$c_{u,nc}$ [kPa]
Stiff silt			
1.0	1080	497	448
1.4	1512	696	624
2.0	2160	994	885
4.0	4320	1987	1750
Average of $(c_u/\sigma'_1)_{nc}$			= 0.41
Soft silt			
1.0	80	42	31
1.4	112	58	43
2.0	160	83	60
4.0	320	166	120
Average of $(c_u/\sigma'_1)_{nc}$			= 0.38

Table 2: Strength and stiffness parameters for the soft and stiff soil.

Silt type		Soft	Stiff
c_u	[kPa]	56	475
ϕ'	[°]	29	33
ψ	[°]	0	3
c'	[kPa]	1	15
E_{50}	[MPa]	3.8	10.2
E_{oed}	[MPa]	5	14
E_{ur}	[MPa]	11.4	30.6
m	[-]	0.5	0.5
$\gamma_{0.7}$	[mm/m]	0.19	0.19
ν	[-]	0.29	0.26
G_0	[MPa]	77.8	102.4
K_0	[-]	0.52	0.46

4 Numerical Modelling

PLAXIS 3D AE is used to compute p-y curves for silt. In total three parameters are changed; drainage type, silt type and diameter of the bucket. The length of the bucket is set to $L/D = 1$. Thereby a total of 12 numerical models are studied, cf. Table 3.

Table 3: Model overview.

Model no.	Drainage type	D and L [m]	Silt type
1	Drained	10	Soft
2	Drained	15	Soft
3	Drained	20	Soft
4	Drained	10	Stiff
5	Drained	15	Stiff
6	Drained	20	Stiff
7	Undrained	10	Soft
8	Undrained	15	Soft
9	Undrained	20	Soft
10	Undrained	10	Stiff
11	Undrained	15	Stiff
12	Undrained	20	Stiff

4.1 Mesh and Model Domain

Correct interpretation of the soil-structure interaction is important, thus interfaces are defined for the bucket, as suggested by both Wolf et al. [2013] and Brinkgreve et al. [2015]. Extended interfaces are needed to be defined for the bottom of the bucket skirt, as recommended by Brinkgreve et al. [2015], as stress concentrations can occur around corners.

A proximity volume, which encloses the bucket is defined, as Østergaard et al. [2015] did. The volume can be given a different mesh density than the rest of the model, as the most intensive shearing occurs closest to the bucket, thereby optimising the calculation time. The mesh density is determined from a convergence analysis, where it is concluded to set the overall coarseness to *medium* and the refinement factor of the proximity volume to *0.16*. From Figure 3 it is possible to see the significant difference in mesh density between the proximity volume and remaining soil volume.

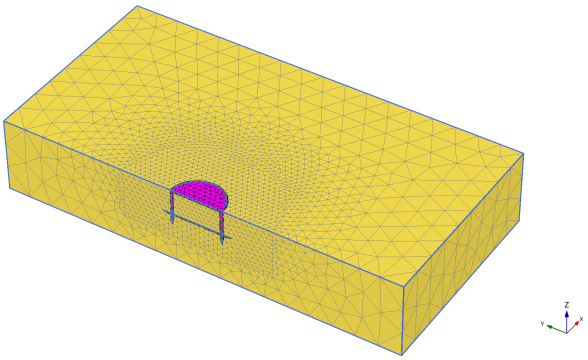

Figure 3: Meshed model.

The size of the model domain is determined from a model domain analysis, as the criteria is, that stresses cannot have a significant affect at the edges. The size of the model domain normalised to the geometry of the

bucket is shown in Figure 4, where the size of the bucket and extended interfaces are shown as well.

4.2 Modelling of Suction Bucket

The thickness of the bucket and Young's modulus is set to 0.3 m and 600.000 MPa, which is considered enough to avoid deflection of the bucket, as only soil response is of interest.

The foundation of a wind turbine is in reality loaded with a horizontal and moment load, which results in rotation of the foundation. Wolf et al. [2013] showed, that calculation complexities arise due to rotation points, which differs from load case to load case. Instead Wolf et al. [2013] suggest the use of a total lateral loading, when examining p-y curves, as only lateral displacements and the associated soil pressure is of interest. Therefore, the models will only be applied with a horizontal displacement with the use of the predescribed displacement function in PLAXIS. Furthermore, only half of the bucket is modelled due to symmetry of geometrical and load conditions, thereby saving calculation time.

4.3 Calculation Phases

The numerical models have five basic calculation phases: The first phase is the *initial phase* (Phase 0), where the initial stress-state of the soil is set with a K_0-procedure. Thereafter the structure is installed in the soil (Phase 1). As the installation can cause displacements, they are reset (Phase 3). Afterwards the bucket is displaced in the amount of the predescribed displacement (Phase 4). Lastly the bucket is unloaded (Phase 5). The two latter phases are repeated with increasing displacement for each load step, until the soil fails or the maximum predescribed displacement is reached.

4.4 Data Extraction and Integration of Stresses

The displacements, y, are extracted from the unloading phases, as the plastic deformation is wanted. This can directly be extracted from PLAXIS, while it is not possible to directly extract the soil pressure, p. The data is instead given as stresses, thus they have to be integrated over an area to obtain the soil pressure. The stresses are extracted from the load phases.

The stresses can either be extracted from the soil elements, or the interface elements defined between the soil and skirt. The latter is used for extraction of stresses, as Wolf et al. [2013] analysed the precision of the different extraction methods, where stresses from the interface elements provided the most precise results.

When the bucket is laterally displaced, the soil moves laterally, thus occurrence of a normal stress, σ'_N, and a shearing stress, τ_1, working around the pile, arise, cf. Figure 5. The figure also shows the occurrence of a second shear stress, τ_2, which works vertically along the skirt, but it is disregarded, as only the lateral soil pressure is of interest. Hence, the soil pressure is calculated by integration of σ'_N and τ_1, as shown in Eq. (4).

$$\int_A = \left(\sigma'_N \sin\theta + \tau_1 \cos\theta\right) dA \tag{4}$$

The bucket skirt is divided into a number of horizontal slices, which describes a depth layer, and vertical slices, hence multiple areas are defined, cf. Figure 6. The stresses within each of the areas, e.g. the black marked area in Figure 6, are averaged and multiplied by the area. Lastly all areas within the same layer (horizontal slice) are summed and divided by the height of the layer to obtain the soil pressure, p.

5 Formulation of p-y Curves for Silt

To develop p-y curves for silt, four steps are taken:

1. Plot of p-y curves from the numerical models, where the data is trimmed for edge effects.
2. Normalise the soil pressure, p, and the displacement, y, with the ultimate soil pressure, p_u and diameter of the bucket, D, respectively.
3. Fitting of FE data to a mathematical function.
4. Define a p-y formulation based on the normalisation and fitted function.

5.1 Step 1: Plot for p-y Curves

Figure 7 and 8 show the plot of the p-y curves for Model 5 and 11 respectively. Each curve refers to a depth, z, which is defined as the middle of each layer. Furthermore, there is significant difference between the drained and undrained behaviour. All the drained models reaches a plateau in the end, while all undrained models reaches a peak in soil pressure before it drops for further displacement. Due to the behavioural difference, the drained and undrained models will be processed separately.

5.2 Step 2: Normalisation of p-y Curves

The displacement is normalised to the diameter of the bucket, D. As seen from Figure 7 and 8 the soil pressure increases with the depth, thus the normalisation should make the curves depth-independent. It is achieved by normalising the soil pressure to the ultimate soil pressure, p_u. As seen in Figure 9 and 10 the depth-dependency is eliminated, as the p-y curves more or less merge into one single curve.

5.2.1 Formulation of Ultimate Soil Pressure

An analysis of the FE data is performed to determine a formulation for p_u. As the drained and undrained silt

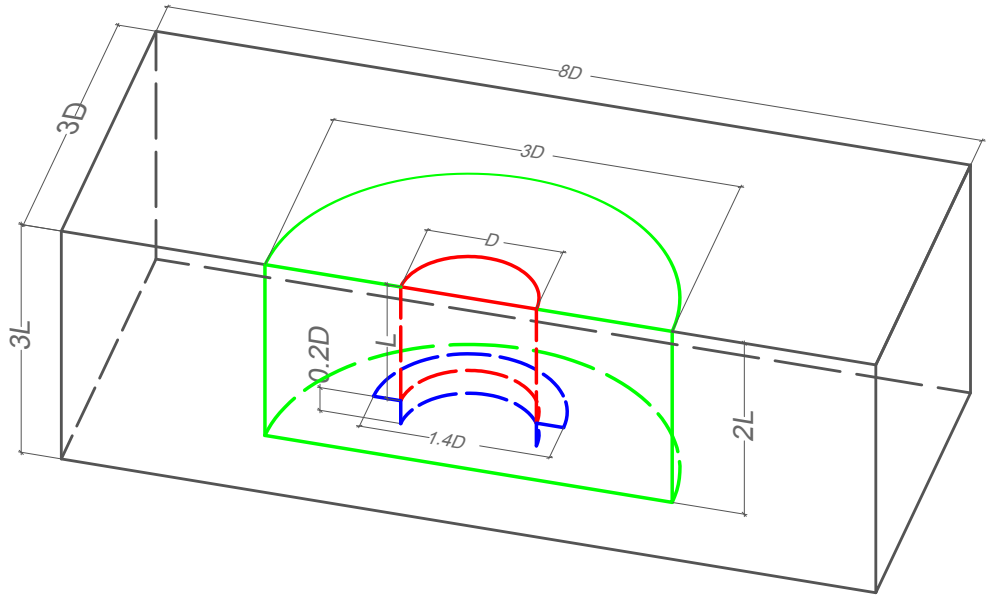

Figure 4: Overall model geometry normalised to the bucket diameter and length. Indication of line colors: black: soil contour/model domain, green: proximity volume with refined mesh, blue: interface extension and red: suction bucket [Østergaard et al., 2015].

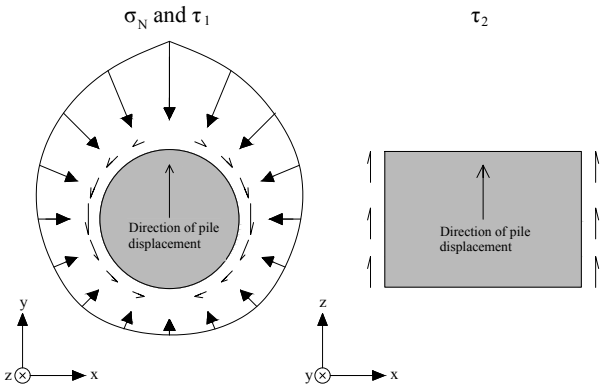

Figure 5: Displacement of pile in y- and z-direction with associating stresses working along the skirt of the suction bucket.

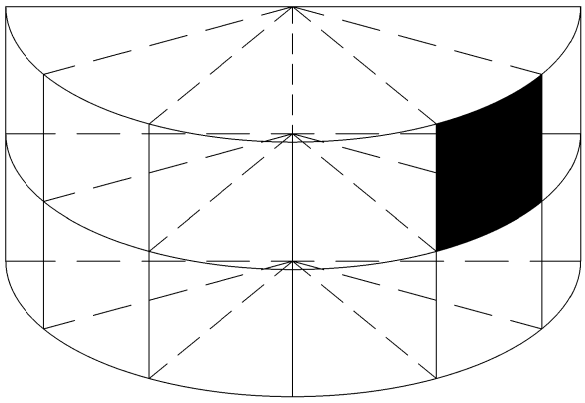

Figure 6: Principle of horizontal and vertical division of the bucket to define integration areas [Østergaard et al., 2015].

are separately processed, formulation will be different as well.

Drained Silt

From the analysis of the drained silt, a good correlation between the values of p_u and $\sigma'_{v0}/(\phi/D)$ is obtained, as seen in Figure 11. The formulation of p_u is given in Eq. (5).

$$p_u = \left(124 \cdot \frac{\sigma'_{v0}}{\phi/D} + 2805\right) \cdot A \qquad (5)$$

Where

$$A = \begin{cases} 0.15 & \text{for soft silt} \\ 1 & \text{for stiff silt} \end{cases}$$

Undrained Silt

The approach to define the p_u for the drained silt is used for the undrained silt as well. The only difference is the correlation, as it is taken between p_u and $\sigma'_{v0}/(c_u/D)$. The analysis shows good correlation, hence the formulation of the ultimate soil pressure for the undrained silt is defined as in Eq. (6).

$$p_u = \left(493 \cdot \frac{\sigma'_{v0}}{c_u/D} + 1843\right) \cdot A \qquad (6)$$

where A is equal to 0.15 and 1 for soft and stiff silt respectively, as for the drained silt.

5.3 Step 3: Fitting of FE data to a Mathematical Formulation

The objective of the third step is to firstly define a mathematical formulation, which describes the normalised p-y curve. The formulation contains model parameters, which afterwards are iterated to fit the normalised p-y curve as well as possible (best fit). The model parameters are free to attain any value.

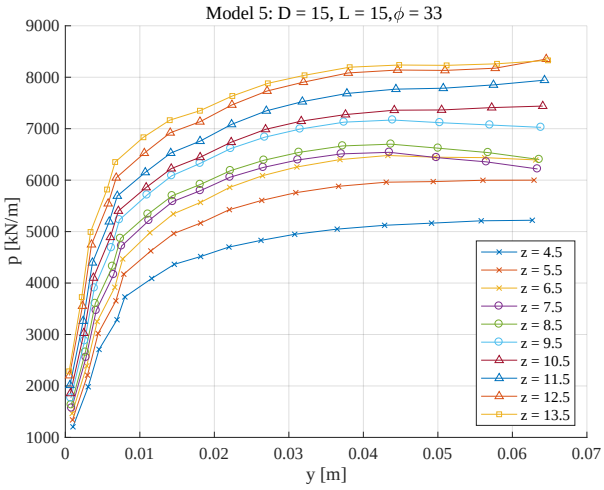

Figure 7: Step 1: Plot of p-y curve for Model 5 with trimmed data.

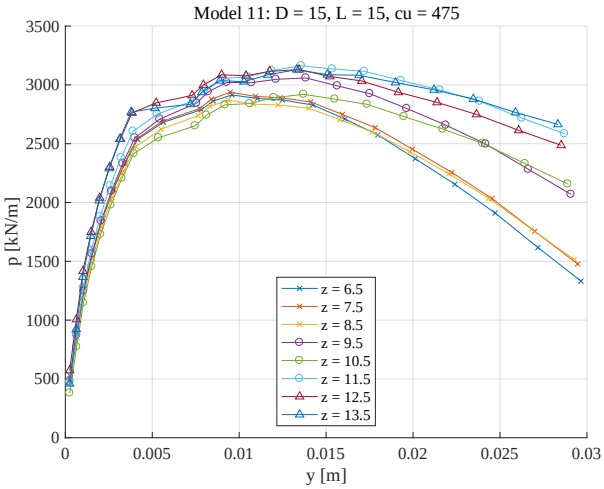

Figure 8: Step 1: Plot of p-y curve for Model 11 with trimmed data.

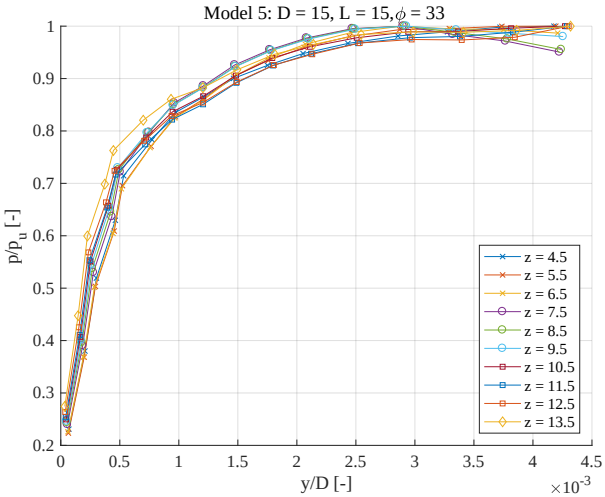

Figure 9: Step 2: Normalised Model 5.

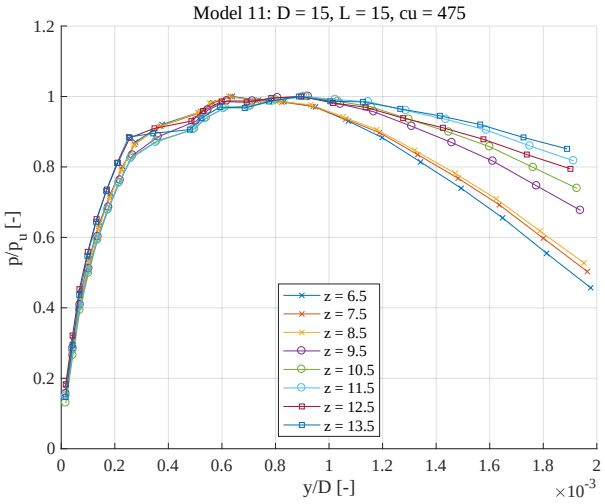

Figure 10: Step 2: Normalised Model 11.

5.3.1 *Fitting of Drained Silt*

The mathematical formulation used to describe the drained silt is given in Eq. (7). β_{1-4} are the model parameters, which are iterated to find the best fit of the normalised FE data. The plot of the best fit for Model 5 is seen in Figure 12.

$$\frac{p}{p_u} = \beta_1 \tanh\left(\beta_2 \frac{y}{D}\right)^{1/3} + \beta_3 \tanh\left(\beta_4 \frac{y}{D}\right)^{1/3} \tag{7}$$

5.3.2 *Fitting of Undrained Silt*

Due to the behaviour of the undrained silt, the p-y formulation is defined differently than for the drained silt, as it is defined in two parts; first part is defined similar to the drained silt, while the second part is defined as a linearly decreasing function, cf. Figure 13. The plot of the best fit for Model 11 is shown in Figure 14, while the intervals and mathematical formulation are defined as:

$$\begin{aligned} 0 \leq y/D < y_B &= 0.0009B \\ y_B \leq y/D < y_C &= 0.002C \end{aligned} \tag{8}$$

$$\begin{aligned} \frac{p}{p_u}\left(\frac{y}{D} < y_B\right) =& \beta_1 \tanh\left(\beta_2 \frac{y}{D}\right)^{1/3} \\ &+ \beta_3 \tanh\left(\beta_4 \frac{y}{D}\right)^{1/3} \end{aligned} \tag{9}$$

$$\begin{aligned} \frac{p}{p_u}\left(\frac{y}{D} = y_B\right) =& \beta_1 \tanh\left(\beta_2 y_B\right)^{1/3} \\ &+ \beta_3 \tanh\left(\beta_4 y_B\right)^{1/3} \end{aligned} \tag{10}$$

$$\frac{p}{p_u}\left(\frac{y}{D} = y_C\right) = 0.75G \tag{11}$$

where

$$B = \begin{cases} 0.4 & \text{for soft soil} \\ 1 & \text{for stiff soil} \end{cases}$$

$$C = \begin{cases} 0.65 & \text{for soft soil} \\ 1 & \text{for stiff soil} \end{cases}$$

$$G = \begin{cases} 0.75 & \text{for soft soil} \\ 1 & \text{for stiff soil} \end{cases}$$

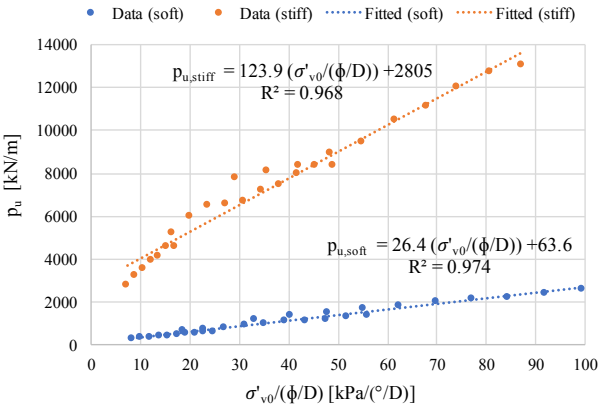

Figure 11: Correlation between p_u and $\sigma'_{v0}/(\phi/D)$ for drained silt.

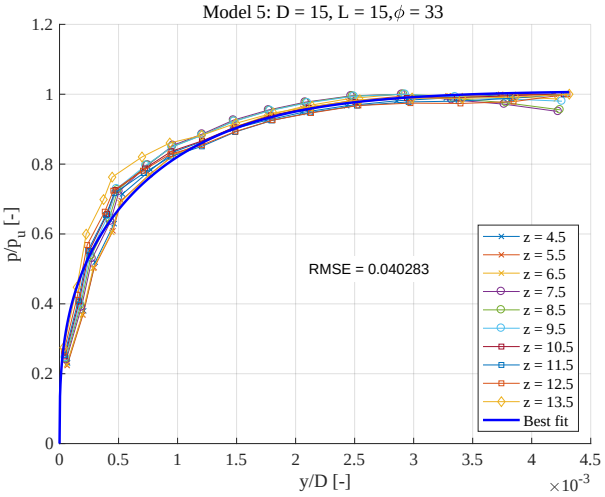

Figure 12: Step 3: Best fit of Model 5 compared to the normalised FE data.

5.4 Step 4: Definition of New p-y Formulation

The only missing part is the formulations for the model parameters, β_{1-4}, as they for the best fit analysis could attain any value. They are sought defined in relation to the soil stiffness, as Vahdatirad et al. [2016] concluded the imprecision in load-displacement estimations were caused by the model parameters, which were defined in relation to the friction angle by Østergaard et al. [2015].

5.4.1 *Formulation of Model Parameters for Drained Silt*

The value of the model parameters from the best fit analysis is plotted against $E_{50}D$, cf. Figure 15-18. In conclusion, the model parameters for the drained silt are defined in Eq. (12).

$$\begin{aligned}
\beta_1 &= 2.2 \cdot 10^{-7} \cdot (E_{50}D) + 0.52 \\
\beta_2 &= 5.97 \cdot 10^{-7} \cdot (E_{50}D)^2 - 0.21 E_{50}D + 1.83 \cdot 10^4 \\
\beta_3 &= 0.45 \\
\beta_4 &= 7.81 \cdot 10^{10} \cdot (E_{50}D)^{-1.55}
\end{aligned} \tag{12}$$

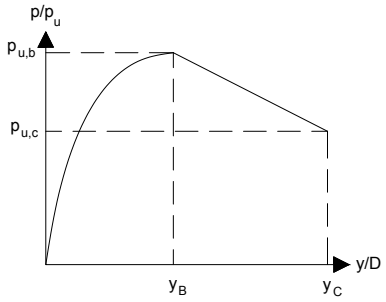

Figure 13: Principle division of p-y curve for undrained silt.

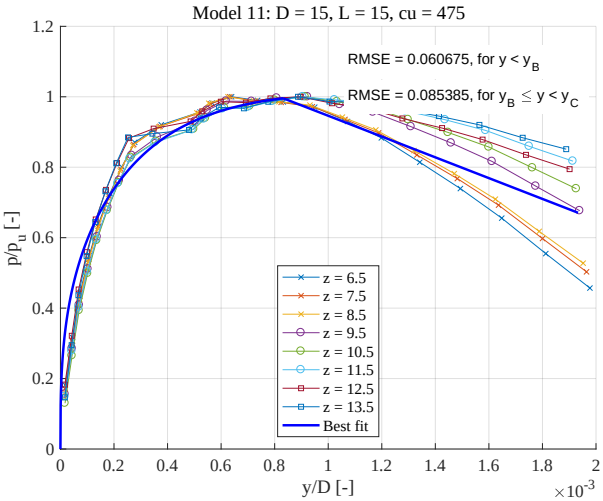

Figure 14: Step 3: Best fit of Model 11 compared to the normalised FE data.

5.4.2 *Formulation of Model Parameters for Undrained Silt*

The model parameters for the undrained silt, given in Eq. (13), are obtained in the same way as for the drained silt.

$$\begin{aligned}
\beta_1 &= 1.91 \cdot 10^{-7} \cdot (E_{50}D) + 0.55 \\
\beta_2 &= 1.93 \cdot 10^{-7} \cdot (E_{50}D)^2 - 0.07 (E_{50}D) + 7970 \\
\beta_3 &= -1.67 \cdot 10^{-7} \cdot (E_{50}D) + 0.47 \\
\beta_4 &= -0.031 (E_{50}D) + 6990
\end{aligned} \tag{13}$$

In Figure 19 and 20 the developed p-y formulation is plotted for the drained and undrained silt for Model 5 and 11 respectively.

6 Formulation of p-y Curves for Sand

Østergaard et al. [2015] made a similar study for drained sand. As the data is available for the study, the same method used to define the p-y formulation for the drained silt is applied to the sand to obtain continuity and simple expressions regardless of soil.

6.1 Step 1-2: Plot and Normalisation of p-y Curves

As for the drained silt, the displacement, y, and soil pressure, p, are normalised to the diameter of the bucket, D, and the ultimate soil pressure, p_u. In Figure 21 and 22 the plot of the p-y curve and normalised p-y curve for

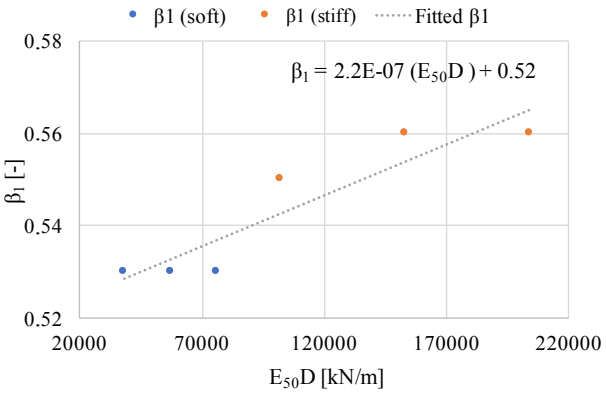

Figure 15: Step 4: Defining model parameter, β_1, in relation to $E_{50}D$ for drained silt.

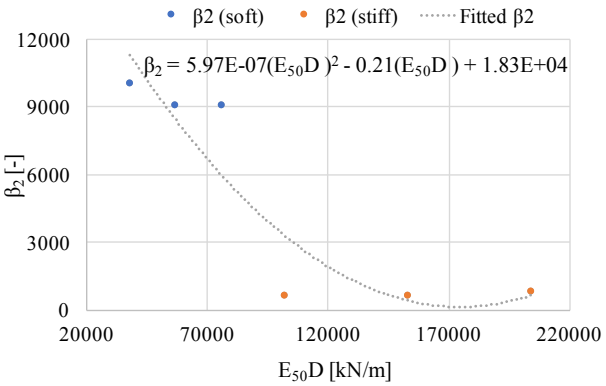

Figure 16: Step 4: Defining model parameter, β_2, in relation to $E_{50}D$ for drained silt.

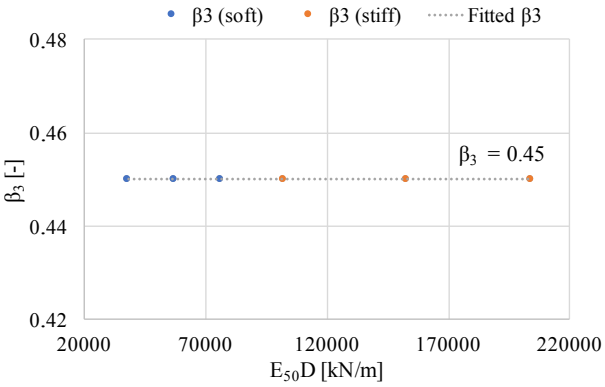

Figure 17: Step 4: Defining model parameter, β_3, in relation to $E_{50}D$ for drained silt.

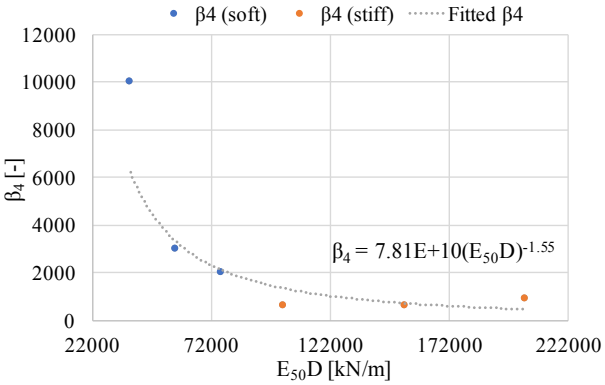

Figure 18: Step 4: Defining model parameter, β_4, in relation to $E_{50}D$ for drained silt.

Model 8 is shown. The use of p_u for normalising p is better, since the p-y curves are more coinciding, compared to normalising with use of the Rankine pressure, p_R, as done in Østergaard et al. [2015].

6.1.1 *Formulation of Ultimate Soil Pressure*

The correlation between p_u and $\sigma'_{v0}/(\phi/D)$ is analysed and shows good correlation for the sand, cf. Figure 23, from which the formulation of p_u is described, cf. Eq. (14).

$$p_u = \left(415\frac{\sigma'_{v0}}{\phi/D} + 169\right)\cdot A \tag{14}$$

where A is defined as:

$$A = \begin{cases} 0.4 & \text{for soft sand} \\ 0.65 & \text{for medium sand} \\ 1 & \text{for stiff sand} \end{cases}$$

6.2 Step 3-4: Fitting of FE Data and Definition of New p-y Formulation

The mathematical expression used to describe the p-y curves for sand is given in Eq. (15), which is identical to the one used for the drained silt.

$$\frac{p}{p_u} = \beta_1 \tanh\left(\beta_2\frac{y}{D}\right)^{1/3} + \beta_3 \tanh\left(\beta_4\frac{y}{D}\right)^{1/3} \tag{15}$$

The FE data is fitted, where β_{1-4} are free to attain any value to fit the data the best way possible. Afterwards the values are plotted against $E_{50}D$, as they are needed in a mathematical expression. The model parameters are defined in Eq. (16), while Figure 24 and 25 show the best fit and mathematical formulation compared to the FE data.

$$\begin{aligned} \beta_1 &= 1.59\cdot 10^{-8}\cdot(E_{50}D) + 0.57 \\ \beta_2 &= -1.18\cdot 10^{-5}\cdot(E_{50}D) + 32.2 \\ \beta_3 &= 3.93\cdot 10^{-8}\cdot(E_{50}D) + 0.52 \\ \beta_4 &= -1.31\cdot 10^{-5}\cdot(E_{50}D) + 23.5 \end{aligned} \tag{16}$$

7 Conclusion

It has been possible to develop p-y formulations by analysing numerical models of lateral displaced buckets in drained and undrained silt. Furthermore, the developed p-y formulation for drained sand showed to be more precise, than the formulation defined by Østergaard et al. [2015], by using the same basic formulation as the drained silt. The governing parameters for the soil pressure for a given displacement were determined to be: the diameter of the bucket, the vertical effective in-situ stress, the soil stiffness and either the friction angle or the undrained shear strength for the drained and undrained soil respectively.

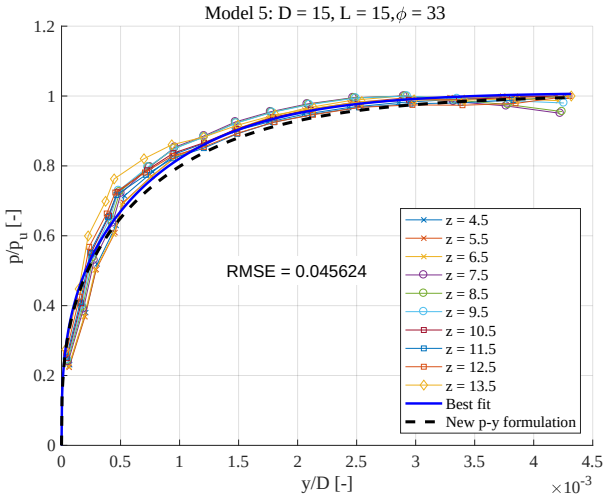

Figure 19: Step 4: New p-y formulation plotted against the best fit and FE data for Model 5.

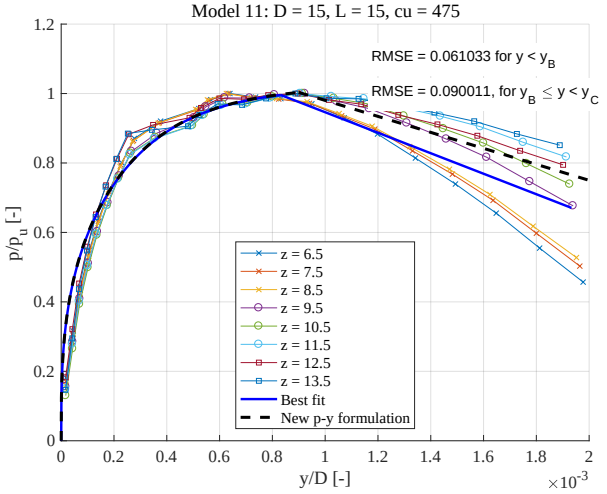

Figure 20: Step 4: New p-y formulation plotted against the best fit and FE data for Model 11.

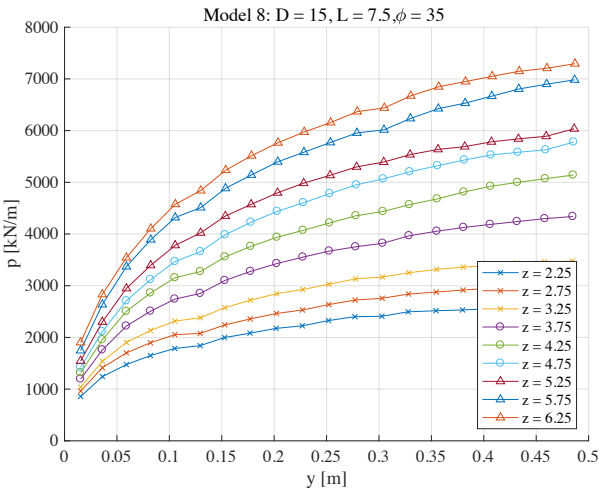

Figure 21: Step 1: Plot of p-y curve for Model 8.

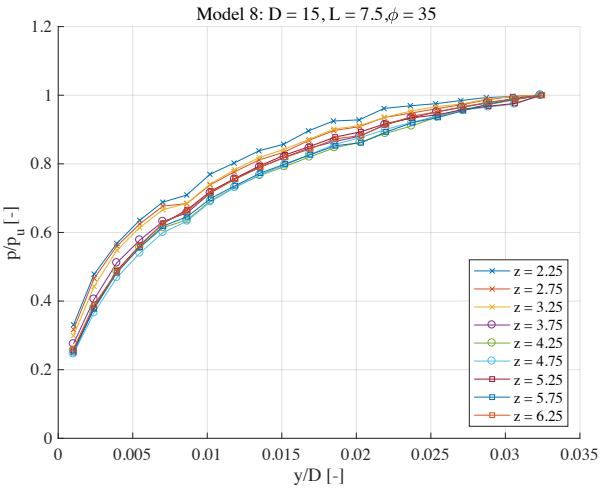

Figure 22: Step 2: Normalisation of p-y curve for Model 8.

The soil stiffness was successfully implemented in the formulations of the model parameters. This was an important objective, as the definition of the model parameters by Østergaard et al. [2015] were believed to cause the imprecision of the soil pressure estimation in Vahdatirad et al. [2016]. Another important outcome of the soil stiffness implementation, was the versatility of the developed p-y formulation, since soils can have different soil stiffnesses for the same friction angle or undrained shear strength, which affects the bearing capacity. These soils are captured by the developed p-y formulations, as the soil stiffness is a governing parameter, whereas the formulation by Østergaard et al. [2015] cannot capture such cases, cf. Figure 26. Thereby, the developed p-y formulations are more versatile, and since they are relative simple and practically applicable for both the silt and sand, it is possible to obtain fast computation of analytical models without compromising on the precision. It is a vital combination to reduce costs and time, hence the objective of the study is considered successfully achieved.

Only a small number of models has been studied, hence it is difficult to implement the formulation in design codes without further evidence of their validation. To validate the formulations, an extension of this study should be to evaluate more numerical models in a bigger spectrum with other strengths of the soil and bucket sizes. As the approach for defining p-y curves for drained silt has shown to be useful for sand as well, another interesting study would be to examine clays. If it is possible to streamline today's different p-y formulations to have the same basic p-y formulations for silts, sands and clays, it would be highly desirable for the sake of simplicity and continuity. If possible, the formulations for silt and sand could be used in a similar study as in Vahdatirad et al. [2016], to compare an analytical model to field tests conducted in similar soil conditions, as the p-y formulations are based on.

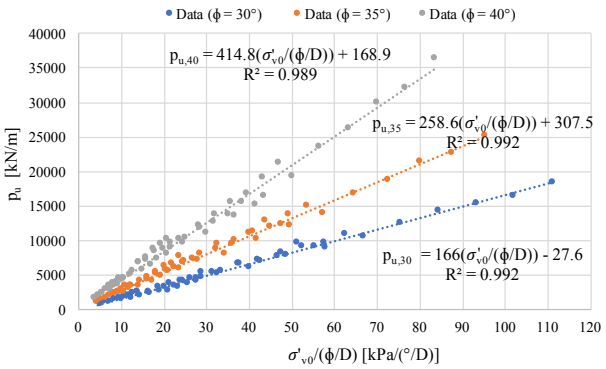

Figure 23: Correlation between p_u and $\sigma'_{v0}/(\phi/D)$ for sand.

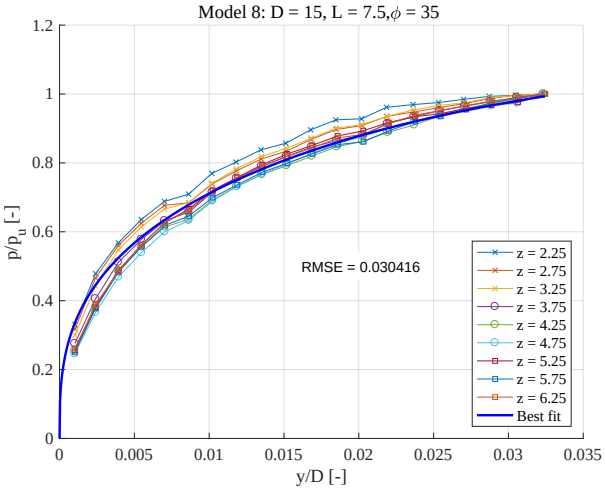

Figure 24: Step 3: Best fit of Model 8 compared to the normalised FE data.

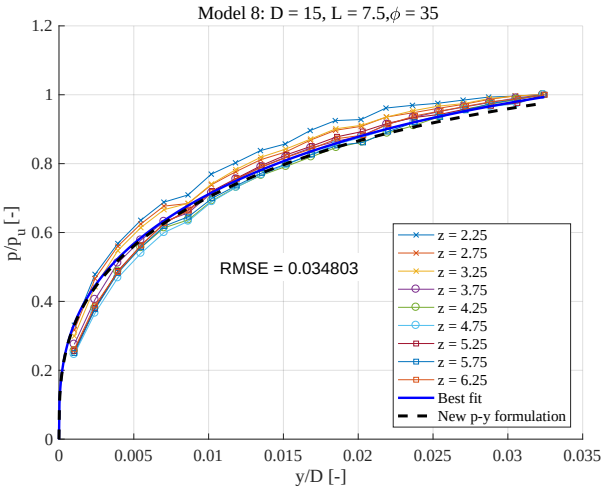

Figure 25: Step 4: New p-y formulation compared to the best fit and FE data for Model 8.

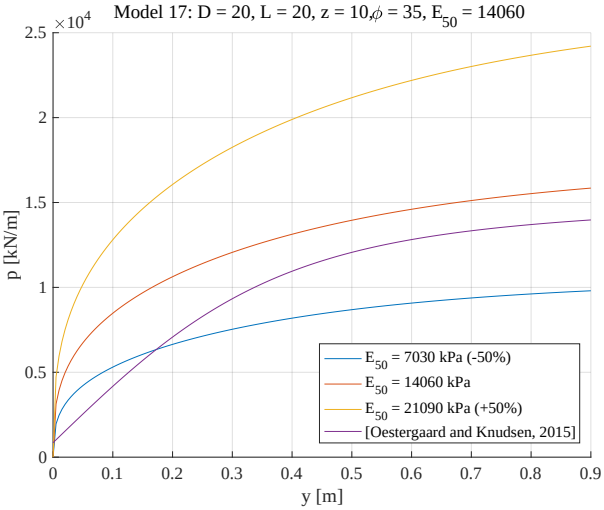

Figure 26: Changing only the soil stiffness $\pm$ 50 % for the developed p-y formulation and the formulation developed by Østergaard et al. [2015].

References

Achmus, Terceros, and Thieken, 2016. Martin Achmus, Mauricio Terceros, and Klaus Thieken. *Evaluation of p-y Approaches for Large Diameter Monopiles in Soft Clay*. ISBN: 978-1-880653-88-3. International Society of Offshore and Polar Engineers, 2016.

Brinkgreve, Kumarswamy, and Swolfs, 2015. R.B.J. Brinkgreve, S. Kumarswamy, and W.M. Swolfs. *PLAXIS 3D Anniversary Edition*. ISBN-13: 978-90-76016-21-4. PLAXIS bv, 2015.

Cox, Reese, and Grubbs, 1974. W. R. Cox, L. C. Reese, and B. R. Grubbs. *Field Testing of Laterally Loaded Piles in Sand*. 1974. Proceedings of the Sixth Annual Offshore Technology Conference, Houston, Texas, paper no. OTC 2079.

Det Norske Veritas, 2013. Det Norske Veritas. *Design of Offshore Wind Turbines*. Det Norske Veritas AS, 2013.

Det Norske Veritas, 1992. Det Norske Veritas. *Foundations - Classification Notes No. 30.4*. Det Norske Veritas AS, 1992.

Jensen, Mohr, Nicolajsen, Mortensen, Bygbjerg, Hansen, Larsen, Hansen, Bager, Svensson, Søndergaard, Plum, Riberholt, Hansen, Dahl, Larsen, Goltermann, Steenfelt, Sørensen, and Bai, 2015. Bjarne Chr. Jensen, Gunner Mohr, Asta Nicolajsen, Bo Mortensen, Henrik Bygbjerg, Lars Pilegaard Hansen, Hans Jørgen Larsen, Svend Ole Hansen, Dirch H. Bager, Eilif Svensson, Ejnar Søndergaard, Carsten Munk Plum, Hilmer Riberholt, Lars Zenke Hansen, Kaare K. B. Dahl, Henning Larsen, Per Goltermann, Jørgen S. Steenfelt, Carsten S. Sørensen, and Werner Bai. *Teknisk Ståbi*. ISBN: 978-87-571-2844-4, 23rd edition. Praxis - Nyt Teknisk Forlag, 2015.

Matlock, 1970. Hudson Matlock. *Correlation for Design of Laterally Loaded Piles in Soft Clays*. ISBN: 978-1-55563-709-5. Offshore Technology Conference, 1970.

Thieken, Achmus, and Lemke, 2015. Klaus Thieken, Martin Achmus, and Katrin Lemke. *A new static p-y approach for piles with arbitrary dimensions in sand*. 2015. in Geotechnik, vol. 38, issue 4, Ernst and Sohn Verlag, pp. 267-288.

Vahdatirad, Diaz, Ibsen, Andersen, Firouzianbandpey, and Griffiths, 2016. Mohammadjavad Vahdatirad, Alberto Troya Diaz, Lars Bo Ibsen, Lars Vabbersgaard Andersen, Sarah Firouzianbandpey, and D. V. Griffiths. *A load-displacement based approach to assess the bearing capacity and deformations of mono-bucket foundations*. 2016. in A Zingoni (ed.), Insights and Innovations in Structural Engineering, Mechanics and Computation: proceedings of the sixth international conference on structural engineering, mechanics and computation, Cape Town, South Africa, 5-7 September 2016. C R C Press LLC, pp. 749-750.

Wolf, Rasmussen, Hansen, Roesen, and Ibsen, 2013. Torben Kirk Wolf, Kristian Lange Rasmussen, Mette Hansen, Hanne Ravn

Roesen, and Lars Bo Ibsen. *Assessment of p-y Curves from Numerical Methods for a Non-Slender Monopile in Cohesionless Soil*. 2013. in The Proceedings of the Twenty-third (2013) International Offshore and Polar Engineering Conference. vol. 2, International Society of Offshore and Polar Engineers, pp. 436-443. International Offshore and Polar Engineering Conference.

Østergaard, Knudsen, and Ibsen, **2015**. Martin Underlin Østergaard, Bjørn Staghøj Knudsen, and Lars Bo Ibsen. *P-y curves for bucket foundations in sand using finite element modeling*. 2015. in V. Meyer (ed.), Frontiers in Offshore Geotechnics III proceedings of the third international symposium on frontiers in offshore geotechnics (isfog 2015), Oslo, Norway, 10-12 June 2015. vol. 1, C R C Press LLC, London, pp. 343-348.

Recent publications in the DCE Technical Memorandum Series

ISSN 1901-7278
DCE Technical Memorandum No. 64